Large-Eddy Simulation of Trailing-Edge Blowing

Jens KRÖMER, Matthias MEINKE and Wolfgang SCHRÖDER

Aerodynamisches Institut
Rheinisch-Westfälische Hochschule Aachen
Wüllnerstr. zw. 5 und 7, 52062 Aachen, GERMANY
Phone: +49-241-80-95410, FAX: +49-241-80-92257,
E-mail: office@aia.rwth-aachen.de

ABSTRACT

A large-eddy simulation of a model flow for trailing-edge blowing as it is often used for cooling turbine blades is carried out to investigate why different wake mixing losses are observed with trailing-edge blowing. The LES is conducted at a free-stream Mach number of M=0.3 and a Reynolds number of Re=18800 based on the free-stream velocity and the trailing-edge thickness. A fully developed turbulent channel flow is used for the trailing-edge jet. The results of the instantaneous turbulent velocity distribution are compared to findings based on a time averaged steady jet at the inflow section. The ratio of the mean velocity of the jet to the free-stream flow at the trailing-edge is about 1.1, so that the Reynolds number based on the friction velocity and half the channel height is $Re_\tau \approx 225$. Vortex structures observed in the different solutions are visualized and wake profiles and turbulence statistics are used to analyze the trailing-edge blowing problem.

INTRODUCTION

Trailing-edge blowing is important in turbine industry, since an improvement in thermal efficiency requires higher turbine inlet temperatures. For conventional turbine blade materials an increase of the inlet temperature can only be achieved by cooling the front stages. The cooling mass flow is usually injected into the wake of the vanes through slots at the trailing-edge. This flow problem has been the subject of many experimental investigations in the past, e.g., Sieverding (1983) or Tabakoff and Hamed (1975) and also of numerical simulations, e.g., Schobeiri and Pappu (1999).

In this paper the results of an LES of the wake of a model problem for a turbine blade with an injected mass flow are presented and the vortex dynamics is investigated to better understand the physical mechanisms why the wake mixing losses depend on the trailing-edge blowing. Since the simulation of a full blade is rather expensive a model problem is considered, where the trailing-edge of a turbine blade is mimicked by a trailing-edge of a flat plate (Fig. 1). Turbulent as well as laminar boundary layers can be prescribed at the outer inlet boundary and a turbulent channel flow is prescribed in the slot from which the trailing-edge jet is emitted.
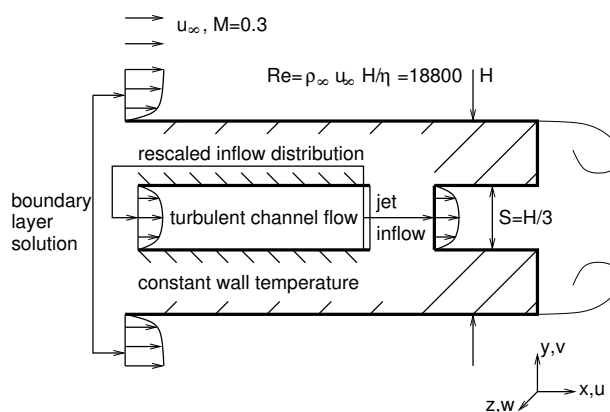

Fig.1: Sketch of the trailing-edge blowing problem to evidence the generation of different turbulent inflow conditions.

The parameters which are common for all presented solutions are given in Table 1. The boundary layer thickness at x=0 is the theoretical value for a flat plate flow at Re_L without being influenced by the acceleration near the trailing-edge, where the Reynolds number Re_L is based on the free-stream values for the density ρ_∞ and velocity u_∞, the length L of the plate and the viscosity η. The Reynolds number Re_τ is based on the friction velocity u_τ and half the channel height $S/2$. These flow parameters correspond to typical values for turbine blades, see e.g., Bohn (1995). The pressure ratio of the stagnation pressure in the slot for the trailing-edge jet and the free-stream pressure $p_{0\text{jet}}/p_\infty$ is chosen such that a jet velocity establishes, which can be expected to generate a minimum of mixing losses downstream of the blade. This velocity ratio has been determined e.g. by Schobeiri and Pappu (1999), who specified a value of $\bar{u}_{\text{jet}}/u_\infty \approx 1.1$ for the ratio of the mean velocity in the jet to the free-stream velocity near the trailing-edge. The above mentioned pressure ratio is fixed for all cases.

To analyze the vortical structures the results of the

different solutions are evaluated using wake profiles of the spatially and time-averaged velocity in the streamwise direction or of the spatially and time-averaged turbulence intensity. To visualize the turbulent vortex pattern of the wake the λ_2-criterion from Jeong and Hussain (1995) is used.

Table 1: Physical parameters for trailing-edge blowing

trailing-edge thickness	$H=1$
trailing-edge jet width	$S=\frac{1}{3}\ H$
boundary layer thickness at $x=0$	$\delta=0.5\ H$
Mach number	$M = 0.3$
Reynolds number Re_H	$\rho_\infty u_\infty H/\eta = 18800$
Reynolds number Re_L	$\frac{L}{H}Re_H = 255000$
Reynolds number in channel Re_τ	$\frac{u_\tau}{u_\infty}\frac{S}{2H}Re_H = 225$
pressure ratio	$p_{0\mathrm{jet}}/p_\infty = 1.064$
velocity ratio	$\bar{u}_{\mathrm{jet}}/u_\infty \approx 1.06\text{-}1.14$
computational domain $x \times y \times z$	$15.5\ H \times 10\ H \times H$

METHOD OF SOLUTION AND BOUNDARY CONDITIONS

The LES is carried out using an explicit scheme for the Navier-Stokes equations formulated for compressible flows. A 5-stage Runge-Kutta method is used for the time integration, the advective fluxes are computed with a modified AUSM scheme in which the pressure derivative is approximated using a centered 5-point stencil to reduce the numerical dissipation. The viscous terms are discretized with a central scheme, so that all spatial derivatives are approximated with second-order accuracy. This scheme is described in detail in Meinke et al. (2002), where the results for free jets and channel and pipe flows indicate that the dissipative truncation error of this scheme can be used as a subgrid scale model. In the literature this method is called the MILES approach. This method is formulated for multi-block structured curvilinear grids and implemented on vector and parallel computers.

For all cases non-reflecting boundary conditions with pressure relaxation (Poinsot and Lele, 1992) are used at outflow boundaries. Since the pressure relaxation introduces some numerical reflections a sponge layer zone is added, in which the source term F is computed as a function of the deviation of the instantaneous solution $q(t)$ from the prescribed solution q_a, $F = \sigma(q(t,\vec{x}) - q_a(\vec{x}))$, where q represents the vector of conservative variables. Here, q_a is simply set to the freestream values. The parameter σ is computed as a function of the distance from the boundaries and increases from zero to σ_{max} within the sponge layer zone. The value for σ_{max} is chosen to be 0.5, which has been determined in test simulations under the condition to minimize numerical reflections. The sponge layer is limited to a zone near the outflow boundaries where $x/H > 8$ and $|y/H| > 4$.

To determine the instantaneous values at the jet inlet

a slicing technique is used. An LES of a fully developed turbulent channel flow is conducted in parallel to the trailing-edge blowing case to provide time accurate turbulent inflow profiles. The results for the fully developed channel flow are discussed in Meinke et al. (2002) and show good agreement with the findings of Kim et al. (1987). In addition, in another computation a steady time averaged turbulent channel flow profile is specified in the trailing-edge slot to investigate the influence of the turbulent structures in the channel on the wake development.

At the inflow boundary above and below the flat plate a zero pressure gradient boundary layer solution is prescribed. At the rigid walls the no-slip condition and a fixed wall temperature are specified. Periodic boundary conditions are applied in spanwise direction.
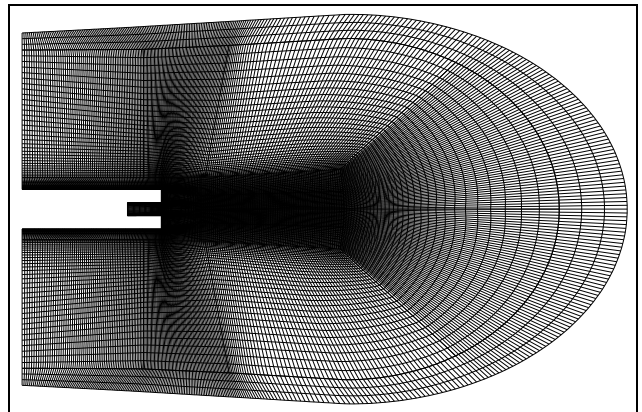

Fig.2: Computational grid in a vertical plane for cases 2 to 4. Every fourth grid point is plotted.
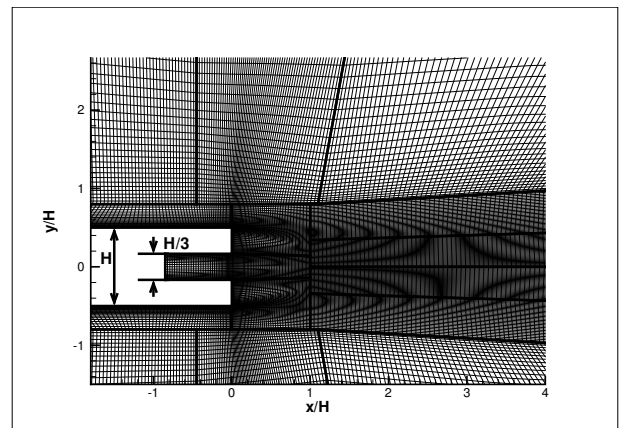

Fig.3: Zoom of the computational grid in a vertical plane for cases 2 to 4. Every second grid point is plotted. Thicker lines indicate block boundaries.

COMPUTATIONAL GRIDS AND INVESTIGATED CASES

The simulations of trailing-edge blowing are carried out on coarse and fine meshes with up to ten million grid points. The characteristic grid parameters for these cases are summarized in Table 2.

The grids for cases 2 to 4 differ only in the spanwise resolution. 65 grid points are used in the spanwise di-

rection for case 4, 49 grid points are used for case 3 and 41 grid points are used for case 2. In case 1 the grid contains 33 grid points in the spanwise direction and is also coarser in the x-y-plane, where only about every second point is used in the wake region. The grid for cases 2 to 4 is shown in Fig. 3

For case 1 and case 2 a steady velocity distribution is used for the jet inflow profile, which is obtained by time averaging the results of the fully turbulent channel flow. Since the wake development depends on the grid resolution and especially on the inflow condition of the jet, the base pressure varies in these solutions resulting in different jet velocities. The variation in the mass flux, however, is small.

Table 2: Inflow condition and grid resolution for the different cases investigated.

	jet inflow condition	grid resolution	grid points
case 1	time averaged channel flow	$\Delta y_{min} = 0.0017\ H$ $\Delta z\quad =\ 0.031\ H$	$3.4 \cdot 10^6$
case 2	time averaged channel flow	$\Delta y_{min} = 0.0015\ H$ $\Delta z\quad =\ 0.025\ H$	$6.2 \cdot 10^6$
case 3	turbulent channel flow	$\Delta y_{min} = 0.0015\ H$ $\Delta z\quad =\ 0.021\ H$	$7.4 \cdot 10^6$
case 4	turbulent channel flow	$\Delta y_{min} = 0.0015\ H$ $\Delta z\quad =\ 0.016\ H$	$9.8 \cdot 10^6$

RESULTS

After the computations have achieved a statistically convergent state, time samples were recorded during 100 time units on the two coarser and about 30 time units on the two finer grids for the determination of statistical data. Here, one time unit corresponds to $\Delta t u_\infty/H$=1.

To study the influence of the grid resolution, streamwise velocity profiles are compared at different locations in streamwise direction for cases 1 and 2 in Fig. 4 and for cases 3 and 4 in Fig. 6, respectively. The streamwise velocity on the centerline y=0 and at y/H=0.33 are shown in Fig. 5 and Fig. 7. For all cases the jet disappears at about x/H=3.5 and a wake like profile develops, since the jet is too weak to compensate for the velocity deficit generated by the trailing-edge.

Although considerable coarser meshes were used for case 1 and case 3 compared to case 2 and case 4, the influence on the velocity profiles is relatively small so that the results on the finer mesh can be regarded as grid independent.

The influence of the boundary condition for the trailing-edge jet can be seen in Fig. 8 and Fig. 9, where profiles of the turbulent kinetic energy are compared for case 2 and case 4. The profiles in wall normal direction show a characteristic double peak due to the two shear layers, which are formed between the external flow and the jet. Significant differences can be observed especially on the centerline of the jet at a location around x/H=1.5 that cannot be explained by the incoming turbulent fluctuations of the channel. These large turbu-
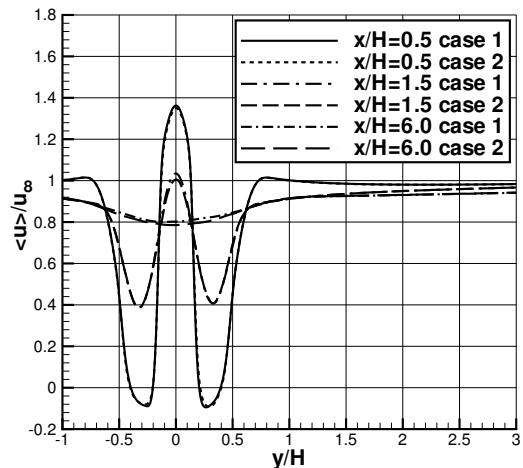

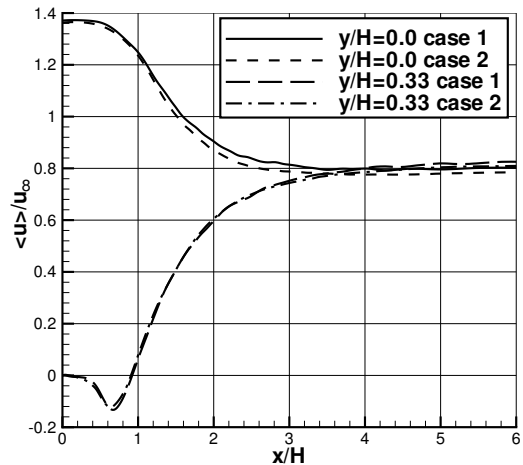Fig.4: Comparison of the streamwise velocity profiles for cases 1 and 2 (steady jet profile).

Fig.5: Comparison of the streamwise velocity profiles for cases 1 and 2 (steady jet profile).

lent fluctuations are generated by a periodical flapping of the jet, which is generated by spanwise vortices in the shear layers. Due to the missing turbulent fluctuations in the channel for the case with a steady jet profile (case 1 and 2) these spanwise vortices are not dissolved as fast as in case 3 and case 4. This can also be seen in the velocity profiles in Fig. 4 and Fig. 6, where the turbulent fluctuations in the channel initiate a faster mixing with the surrounding flow. The development of the turbulent kinetic energy on the centerline in Fig. 9 shows higher peak values and a slower decay for the case with a steady jet profile. This can be explained again with the turbulent fluctuations from the channel in case 4. These fluctuations excite an earlier generation of streamwise vortices and thus reduce the strength of the spanwise rollers, so that the turbulent kinetic energy decays faster in streamwise direction.

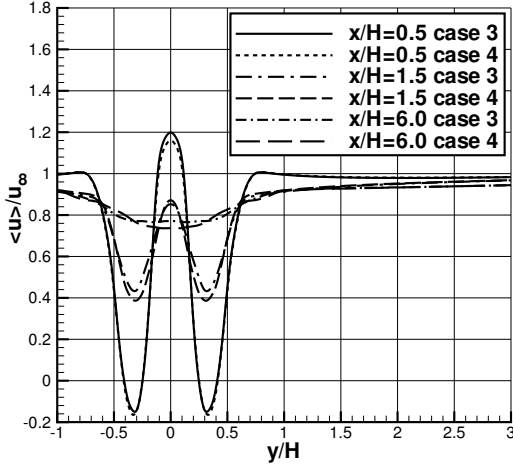From these results it can be concluded that it is neces-

3

Fig.6: Comparison of the streamwise velocity profiles for cases 3 and 4 (instantaneous jet profile).
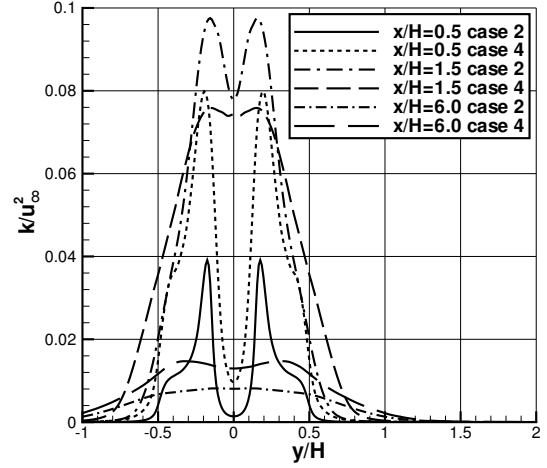

Fig.8: Comparison of the turbulent kinetic energy profiles for cases 2 and 4.
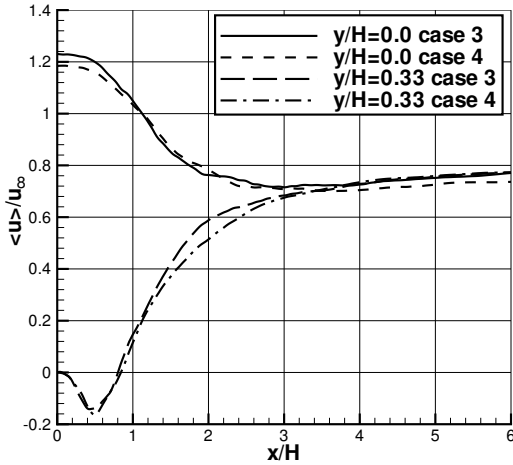

Fig.7: Comparison of the streamwise velocity profiles for cases 3 and 4 (instantaneous jet profile).
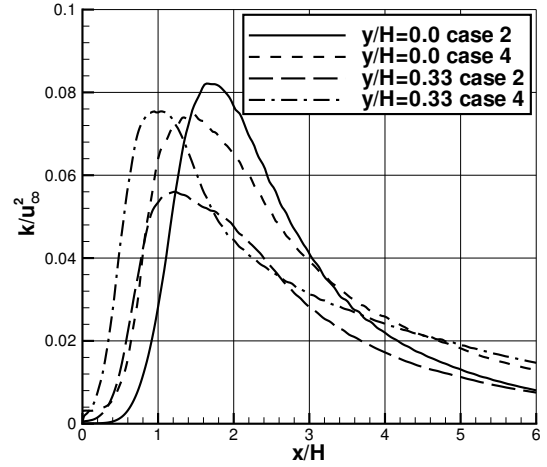

Fig.9: Comparison of the turbulent kinetic energy profiles for cases 2 and 4.

sary to represent the turbulent fluctuations realistically in the LES to capture the correct wake development.

The vortex structures in the wake are visualized with contours of λ_2 according to Jeong and Hussain (1995). Results for a case with similar flow parameters, but without trailing-edge blowing from Opiela et al. (2000) are shown in Fig. 10 and Fig. 13. Strong spanwise rollers connected with streamwise vortices can be seen, which is typical for a turbulent vortex street. The same visualization for case 2 and case 3 in Fig. 11 and Fig. 12 reveals that the wake is not dominated by the spanwise vortices. Such vortices exist only in the very vicinity of the trailing-edge and are dissolved very fast by the turbulent fluctuations in the mixing layer.

Differences can also be observed comparing the results for case 2 and case 3. Due to the missing turbulent fluctuations in the slot emitting the jet, stronger spanwise vortices are shed from the trailing-edge for case 2. In the case with trailing-edge blowing these spanwise vortices are smaller in diameter and occur in all four shear layers behind the trailing-edge.

As a consequence a more slender wake develops. This can be seen in Fig. 13 and Fig. 14 or Fig. 15, where the distribution of the turbulence intensities in the streamwise direction is plotted for a wake behind a rectangular trailing-edge without and with blowing. Note that the same scale is used for these figures. For the case with blowing (Fig. 14 and Fig. 15), there is a narrow and intense region directly behind the trailing-edge, which decays much faster than in the case without blowing (Fig. 13). This discrepancy is clearly due to the fact that the shedding of spanwise vortices is strongly reduced by the trailing-edge jet. The asymmetry of the results in Fig. 15 indicate that the number of samples recorded for this case is not large enough. The tendency, however, is already clearly visible.
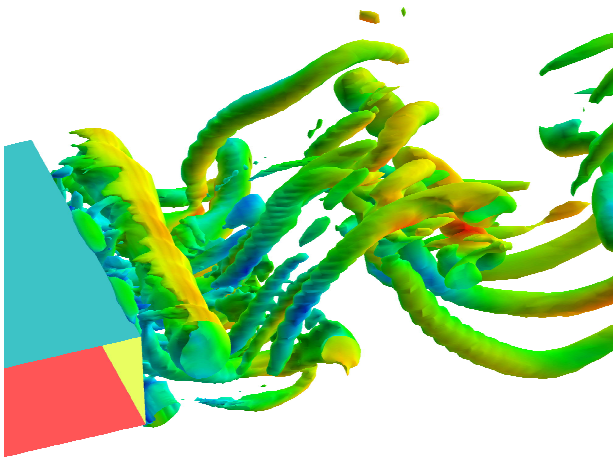
4

Fig.10: Visualization of the vortex structures using λ_2 contours color coded with the local Mach number in the wake without trailing-edge blowing.
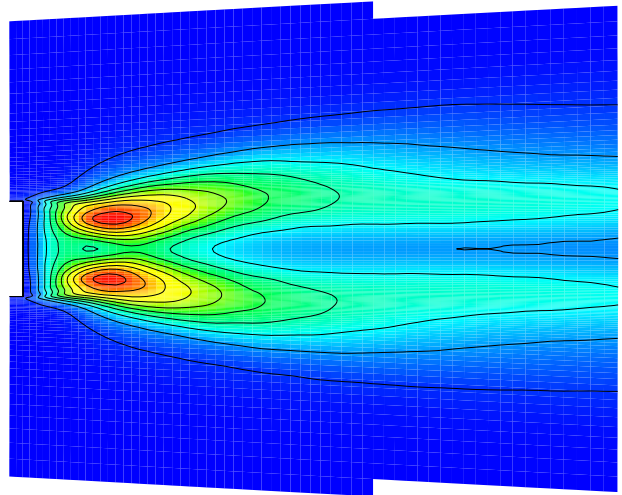

Fig.11: Visualization of the vortex structures using λ_2 contours color coded with the local Mach number in the wake with trailing-edge blowing; case 2.

Fig.12: Visualization of the vortex structures using λ_2 contours color coded with the local Mach number in the wake with trailing-edge blowing; case 3.

Fig.13: Time and spanwise averaged distribution of the Reynolds stress component $u'u'$ in the wake of the rectangular trailing-edge without blowing.
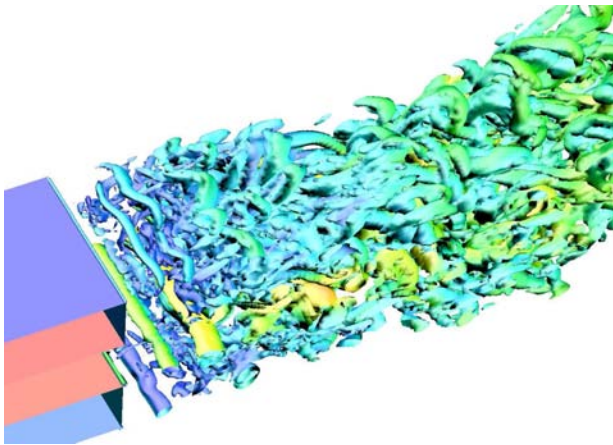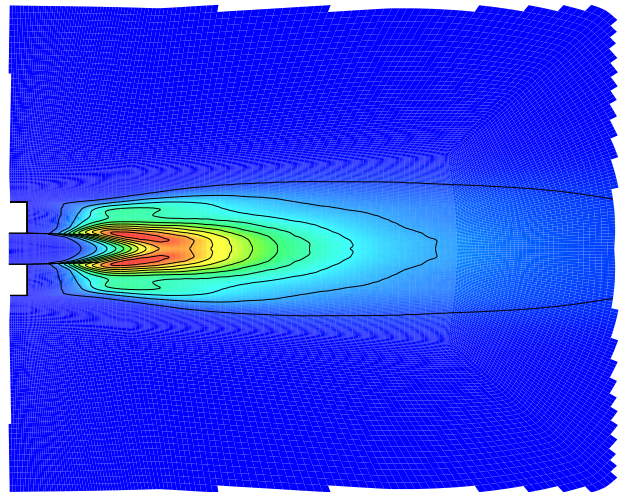

Fig.14: Time and spanwise averaged distribution of the Reynolds stress component $u'u'$ in the wake of the rectangular trailing-edge with blowing for case 2.
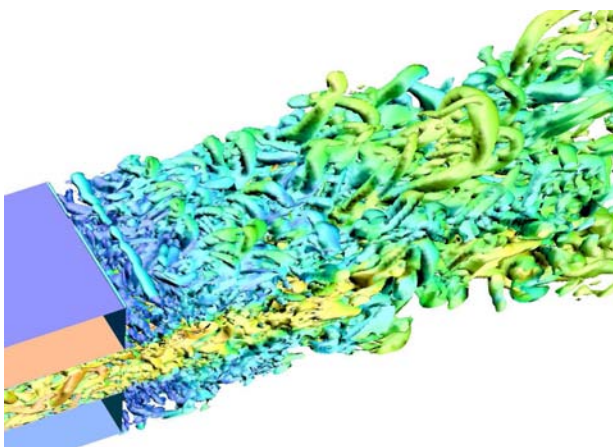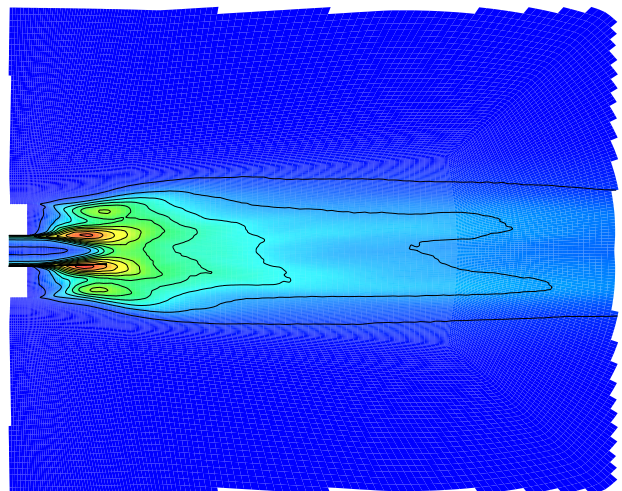

Fig.15: Time and spanwise averaged distribution of the Reynolds stress component $u'u'$ in the wake of the rectangular trailing-edge with blowing for case 4.

CONCLUSION

The simulation of the wake with trailing-edge blowing shows that the jet from the trailing-edge inhibits the shedding of large vortices, which occurs without trailing-edge blowing. Instead, smaller spanwise vortices form especially in the shear layer of the jet, but which are dissolved very fast by the turbulent fluctuations. Since less energy is required for the formation of the smaller vortices and the mixing with the surrounding flow is reduced, the losses in the wake are diminished.

The same investigations are carried out for the case of turbulent boundary layers, for which the inflow profile above and below the plate will be obtained from an already existing LES for a spatially developing boundary layer. In addition, different boundary layer thicknesses can be prescribed at the lower and upper surface. First details of these investigations will be presented at the conference.

References

Bohn, D., Becker, V., Behnke K., and Bonhoff, B., 1995, "Experimental and Numerical Investigations of the Aerodynamical Effects of Coolant Injection through the Trailing Edge of a Guide Vane," ASME paper 95-GT-26, Houston, Texas, USA

Jeong, J., and Hussain, F., 1995, "On the identification of a vortex," *Journal of Fluid Mechanics*, Vol. 285, pp. 69-94

Kim, J., Moin, P., and Moser, R., 1987, "Turbulence Statistics in Fully Developed Channel Flow at Low Reynolds Number," *Journal of Fluid Mechanics*, Vol. 177, pp. 133-166

Meinke, M., Schröder, W., Krause, E., and Rister, T., 2002, "A Comparison of Second- and Sixth-Order Methods for Large-Eddy Simulations," *Computers and Fluids*, Vol. 31, pp. 695-718

Opiela, M., Meinke, M., Schröder, W., Comte, P., and Briand E., 2000, "LES of turbulent boundary layers and wakes," CNRS-DFG Collaborative Research Programme, Vieweg Verlag, Braunschweig

Poinsot, T. J., and Lele, S. K., 1992, "Boundary Conditions for Direct Simulations of Compressible Viscous Flows," *Journal of Computational Physics*, Vol. 101, pp. 104-129

Schobeiri, M. T., and Pappu, K., 1999, "Optimization of Trailing Edge Ejection Mixing Losses: A Theoretical and Experimental Study," *Journal of Fluid Engineering*, Vol. 121, pp. 118-125

Sieverding, C. H., 1983, "The influence of Trailing Edge Ejection on the Base Pressure in Transonic Turbine Cascades," *ASME Journal of Engineering for Power*, Vol. 105, pp. 215-222

Tabakoff, W., and Hamed, A., 1975, "Theoretical and Experimental Study of Flow through Turbine Cascades with Coolant Flow Injection," AIAA Paper 75-843